SCIENTIFIC REPORTS

OPEN

SUBJECT AREAS:
PERMEATION AND TRANSPORT
PATCH CLAMP
HIGH-THROUGHPUT SCREENING
ASSAY SYSTEMS

Received
21 December 2012

Accepted
21 January 2013

Published
6 February 2013

Correspondence and requests for materials should be addressed to M.P. (pusch@ge.ibf.cnr.it)

An optical assay of the transport activity of ClC-7

Ilaria Zanardi, Giovanni Zifarelli & Michael Pusch

Istituto di Biofisica, CNR, Via De Marini 6, 16149 Genoa, Italy.

Osteoporosis, characterized by excessive osteoclast mediated bone resorption, affects millions of people worldwide representing a major public health problem. ClC-7 is a chloride-proton exchanger localized in lysosomes and in the resorption lacuna in osteoclasts where it is essential for bone resorption. Thus, drugs targeted at ClC-7 have been proposed for ameliorating osteoporosis. However, functional assays suited for high throughput screening (HTS) of ClC-7 function are lacking. Here we describe two complementary variants of purely optical assays of the transport activity of ClC-7, redirected to the plasma membrane employing a genetically encoded fluorescent Cl^-/pH indicator fused to the ClC-7 protein. These simple and robust functional assays of ClC-7 transport are well-suited to be applied in HTS of small-molecule inhibitors and may help to develop drugs suited for the treatment of osteoporosis.

Osteoporosis, characterized by excessive osteoclast mediated bone resorption, affects millions of people worldwide with predominance in women and elderly people, becoming a major public health problem[1]. The increase in the proportion of elderly people will have a dramatic impact on health care costs since it is expected that the number of osteoporotic fractures will double over the next 50 years[1]. In osteoporosis an imbalance of osteoblast mediated bone formation and osteoclast mediated bone resorption leads to progressive loss of bone mass and results in bone fragility[2]. Bone resorption is directed by osteoclasts that release protons and proteases in the resorption lacunae causing the dissolution of hydroxyapatite, and the cleavage of matrix proteins[3]. The acidification of the resorption lacunae, as in lysosomes, depends on chloride. Chloride ions have been proposed to maintain the electro-neutrality providing negative charges when protons are released in the lacuna and permits an efficient decrease of pH[4], but the precise role of the Cl^- transport into the resorption lacuna is not clear[5]. Several approaches for the treatment of osteoporosis are currently available[6] allowing diverse therapy strategies but initially rather effective treatments are associated sometimes with unwanted side-effects[7]. Thus, novel effective drugs for the treatment of osteoporosis may have a significant positive impact. A promising pharmacological target is the lysosomal Cl^-/H^+ exchanger ClC-7 [8]. Loss of function of ClC-7, or of its associated beta subunit Ostm1, in man and mice lead to osteopetrosis, neurodegeneration and lysosomal storage disease[9–13]. The osteopetrotic phenotype is explained by the fact that the ion transport activity of ClC-7 is essential for the osteoclast mediated bone resorption. Conversely, osteoporosis is caused by excessive bone resorption. Thus, reducing bone resorption by blocking ClC-7 activity can be expected to provide a highly effective treatment of osteoporosis[8].

ClC-7 associated with Ostm1 is an intracellular chloride-proton exchanger member of the CLC protein family localized in lysosomes and in the ruffled border of osteoclasts. Among anion-transporting CLC proteins some function as passive Cl^- channels and others work as active anion/proton antiporters with a stoichiometry of two-anions: one-proton[14,15]. Human ClC-1, ClC-2, ClC-Ka, and ClC-Kb, are chloride ion channels expressed on the plasma membrane, whereas ClC-3, ClC-4, ClC-5, ClC-6, and ClC-7 are intracellular Cl^-/H^+ antiporters localized mostly in endosomal and lysosomal membranes[16].

The lysosomal localization of ClC-7 precludes a classic electrophysiological approach for the investigation of its functional characteristics. Recently, however, the disruption of a leucine motif within the cytoplasmic N-terminus resulted in a partial plasma membrane redirection of the transporter[17]. Exploiting this mutation, allowed Leisle et al.[18] to characterize the biophysical properties of ClC-7 revealing a slow voltage dependent activation at voltages more positive than ~20 mV and establishing a $2Cl^-/1H^+$ exchange stoichiometry similar to ClC-4 and ClC-5, the prokaryotic ClC-ec1 and the nitrate/proton antiporter AtCLCa[19–22].

Even though electrophysiology can be used to sharply investigate the characteristics of ion transporting membrane proteins, it is a time-consuming and labor-intensive technique and it is unlikely to be exploited in high throughput screening (HTS). An acid influx assay monitoring the effect of activation of the V-ATPase, in the

presence of the potassium ionophore valinomycin (VAL) on human osteoclasts expressing ClC-7 was recently developed by Jensen et al.[23]. However, the complications related to the specific cell line required and the elaborate osteoclast membrane vesicle preparation render also this method hard to be used in HTS.

Here, we describe a purely optical assay of ClC-7/Ostm1 function employing the E²GFP/DsRed Cl^-/pH sensor[24] fused to the C-terminus of ClC-7. The assay can be easily miniaturized and transformed for a use in HTS.

Results

Localization and functionality of Ostm1-2AP-wtClC-7^{PM}-E²GFP/DsRed and Ostm1-2AP-E245A-ClC-7^{PM}-E²GFP/DsRed. In order to develop a functional optical assay of the ClC-7 transporter we exploited the recently developed GFP-based biosensor E²GFP/DsRed, which allows to measure simultaneously the concentration of protons and Cl^- ions, employing fluorescence excitation at three different wavelengths[24]. The sensor is a fusion of two independent fluorophores: a pH and [Cl^-] sensitive GFP variant (E²GFP) and the pH and Cl^- insensitive red fluorescent DsRed[24]. In order to reduce the number of constructs to co-express, and to localize the Cl^-/H^+ sensor as close as possible to the transporter itself, we fused the E²GFP/DsRed sensor to the cytoplasmic C-terminus of ClC-7, which did not alter the functional properties of ClC-7 (see below). WT ClC-7 strictly localizes to lysosomes/late endosomes[5,10,11] but recently Stauber et al.[17] identified an N-terminal leucine based sorting motif that, when mutated (L23A-L24A-L36A-L37A; "ClC-7^{PM}") redirects a significant proportion of the transporter to the plasma membrane and renders it more accessible for functional studies[17,18]. Consequently, we introduced these mutations in the

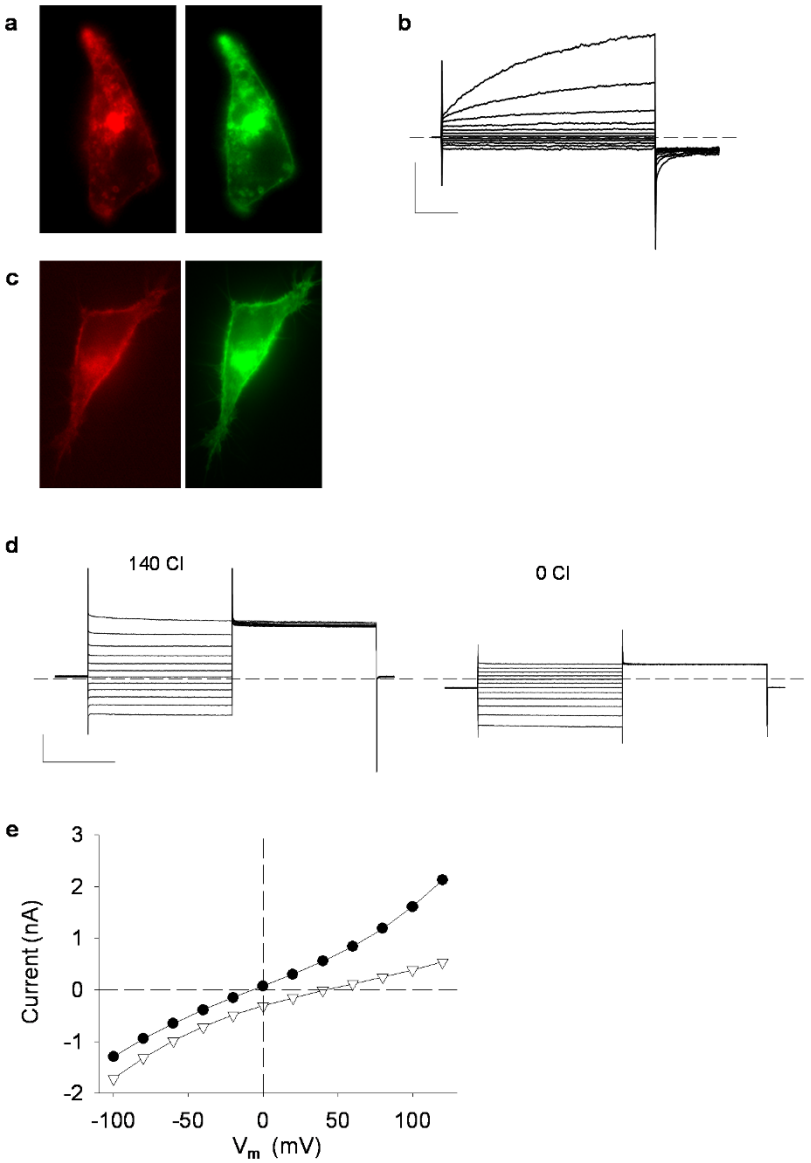

Figure 1 | Ostm1-2AP-wtClC-7^{PM}-E²GFP/DsRed and Ostm1-2AP-E245A-ClC-7^{PM}-E²GFP/DsRed are localized in the plasma membrane and are functional. (a) DsRed (red) and E²GFP (green) fluorescence in cells transiently transfected with Ostm1-2AP-wtClC-7^{PM}-E²GFP/DsRed. (b) typical whole-cell currents from Ostm1-2AP-wtClC-7^{PM}-E²GFP/DsRed transfected HEK293 cells recorded using patch-clamp technique. Vertical scale bar represent 1 nA, horizontal 200 ms. (c) fluorescence of DsRed (red) and E²GFP (green) partially localizes in the plasma membrane in Ostm1-2AP-E245A-ClC-7^{PM}-E²GFP/DsRed transfected cells. (d) patch-clamp recordings of characteristic whole-cell currents elicited from Ostm1-2AP-E245A-ClC-7^{PM}-E²GFP/DsRed expressing cells in the presence of 140 mM Cl in the external solution (top panel), and after removal of extracellular chloride (bottom panel). Vertical scale bar represent 1 nA, horizontal 200 ms.

constructs for our assay. Functional expression of ClC-7 requires the presence of the beta subunit Ostm1[12,18,25]. To additionally reduce the number of different cDNAs to transfect and to ensure the simultaneous and equivalent expression of ClC-7P^{PM}-E^{2}GFP/DsRed and Ostm1, we constructed a plasmid in which the two cDNAs are linked by a self-cleavable 2A peptide. The 2A peptide mediates a co-translational cleavage producing multiple proteins from a polyprotein encoded by a single open reading frame[26].

The resulting construct (Ostm1-2AP-wtClC-7^{PM}-E^{2}GFP/DsRed) was fully functional in *Xenopus* oocytes (Supplementary Fig. 1) and in transfected HEK cells (Fig. 1) showing the expected partial plasma membrane expression of the fusion protein (Fig. 1a). Transfected HEK cells were also tested for functional expression using the patch-clamp technique yielding slowly activating outwardly rectifying currents at positive voltages >= 20 mV as described by Leisle *et al.*[18] (Fig. 1b).

The strong voltage-dependence poses a severe problem for a non-electrophysiological assay of ClC-7 function, because it is not trivial to clamp the plasma membrane at a positive voltage, for example by using ionophores or K-depolarization, which results at most in a voltage around 0 mV. To circumvent this problem, we adopted two different strategies. In a first approach, we additionally introduced a mutation of the gating glutamate (E245A) which renders the transporter voltage-independent and which abolishes proton transport[18]. Also this construct (Ostm1-2AP-E245A-ClC-7^{PM}-E^{2}GFP/DsRed) was fully functional in oocytes (Supplementary Fig. 2) and in transfected HEK cells (Fig. 1c, d). The outwardly directed current component was abolished when the extracellular chloride was removed and a shift of the reversal potential to more positive values was observable as expected from a chloride-selective current and in agreement with previous studies (Fig. 1e)[18]. These constitutive, voltage-independent currents of the gating glutamate mutant render it amenable to the Cl^- flux assay described below.

Development of the Cl^- flux assay exploiting ClC-1 transport activity. In order to be able to test the Cl^- flux assay with a blocking compound we first screened several commonly used chloride channel blockers on the gating glutamate mutant (E245A) expressed in *Xenopus* oocytes. Unfortunately, none of these compounds showed inhibitory activity with an EC-50 below 0.5 mM (Supplementary Table 1) with the most potent substance being RT-93[27], which has an EC-50 of 0.8 mM, too large to be useful as a test compound.

Thus, in the absence of a suitable positive control, we set-up the assay using as a surrogate the plasma membrane localized ClC-1 chloride channel[28] which is specifically blocked by 9-anthracene carboxylic acid (9-AC)[29]. As for ClC-7, E^{2}GFP/DsRed was fused to the cytoplasmic C-terminus of ClC-1 (Fig. 2a) and the functional expression of the channel in transiently transfected HEK293A cells was controlled using the patch-clamp technique (data not shown). As a negative control we transfected HEK293A cells with the soluble E^{2}GFP/DsRed sensor localizing in the cytoplasm (Fig. 2b).

The basic idea of the assay is to abruptly reduce the extracellular chloride concentration ($[Cl^-]_{ext}$) and to monitor the resulting ClC-1 mediated decrease of the intracellular chloride concentration ($[Cl^-]_{int}$) that leads to an increase of the E^{2}GFP fluorescence (via a reduced static quenching) by measuring the E^{2}GFP/DsRed fluorescence ratio. A critical feature of the assay is to carefully adjust the osmolarity of the solutions (by adding mannitol) to avoid the activation of endogenous volume regulated anion channels (VRAC)[30]. In order to provide a sustained driving force for chloride exit the potassium ionophore valinomycin (VAL) was added to the solutions.

Fluorescence was excited a 458 nm and 482 nm (for E^{2}GFP) and 563 nm (for DsRed) and emission of the E^{2}GFP fluorescence and DsRed fluorescence was split using a dual view configuration (Till photonics) and images were recorded with a EXI Blue camera

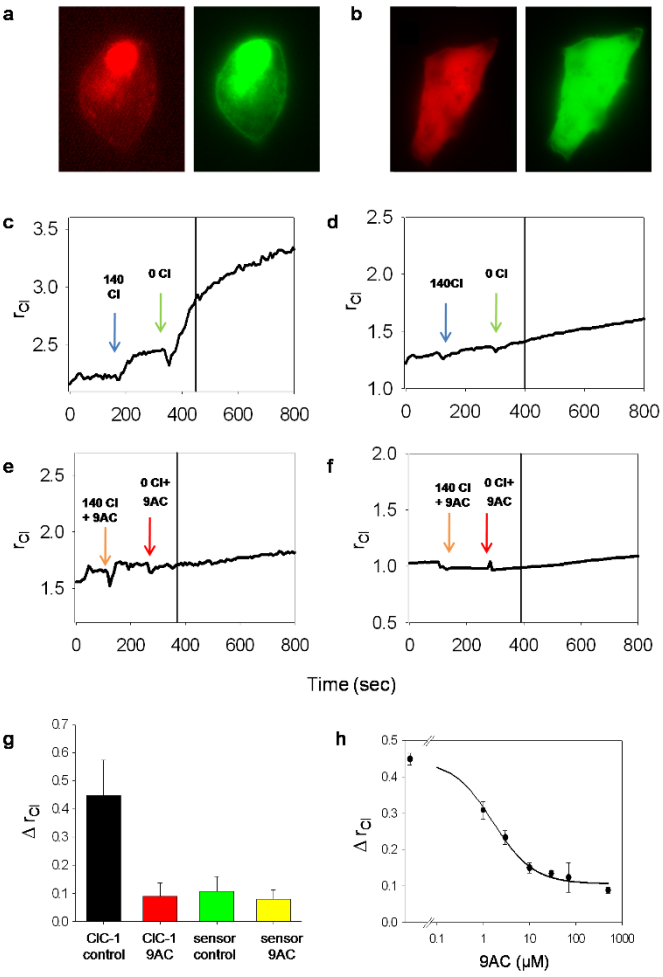

Figure 2 | Cl^- flux assay detects ClC-1 transport activity. Plasma membrane localized fluorescence of DsRed (red) and E^{2}GFP (green) in ClC-1-E^{2}GFP/DsRed transfected HEK cells (a) and cytosolic diffused fluorescence in cells transfected with soluble E^{2}GFP/DsRed (b). Effect of the change in $[Cl^-]_{ext}$ from 140 mM to 0 mM on r_{Cl} on a single cell expressing ClC-1-E^{2}GFP/DsRed (c) or soluble E^{2}GFP/DsRed (d). Effect of 500 µM 9-AC on the change in r_{Cl} in cells expressing ClC-1-E^{2}GFP/DsRed (e) or soluble E^{2}GFP/DsRed (f). Here and in all following figures, arrows indicate times of the solution change; vertical lines mark 100 s after the preceding solution change. Mean values of the change of r_{Cl} at 100 seconds after the start of the perfusion with the 0 Cl solution (g). Dose response analysis of the effect of 9-AC on r_{Cl} in ClC-1 expressing cells (0 µM 9-AC: n = 67; 1 µM 9-AC: n = 18; 3 µM 9-AC: n = 27; 10 µM 9-AC: n = 25; 30 µM 9-AC: n = 25; 70 µM 9-AC: n = 4; 500 µM 9-AC n = 36; Error = SEM) (h).

(QImaging Retiga). Images were recorded at ~0.1 Hz while the transfected cells were exposed to a drop in $[Cl^-]_{ext}$ (from 140 mM to 0 mM, in the continued presence of 100 µM valinomycin). In order to optimize the throughput of the screening assay using the iMIC microscope we exploited the possibility of the system to memorize a large number of positions (x-y-z) of the microscope stage (x-y) and objective height (z), to be able to scan a relatively large number of cells from the same culture dish, each at the single cell level. Following the abrupt decrease in $[Cl^-]_{ext}$ we observed a gradual increase of r_{Cl} (r_{Cl} = F458/F563) in ClC-1-E^{2}GFP/DsRed expressing cells (Fig. 2c) but not in cells transfected with the soluble E^{2}GFP/DsRed (Fig. 2d). Addition of 9-AC (500 µM), a specific blocker of ClC-1, eliminated the fluorescence increase in ClC-1 transfected cells (Fig. 2e) and had no effect in E^{2}GFP/DsRed expressing cells (Fig. 2f). To quantify the fluorescence changes we calculated the change of r_{Cl} at 100 seconds after the start of the perfusion with the 0 Cl solution

(Fig. 2g). A dose response analysis of the blocking effect of 9-AC (Fig. 2h) was conducted revealing an EC-50 value of ~1.6 μM, in good agreement with electrophysiological results[29]. These results confirm that the fluorescence change reflects specific chloride transport through ClC-1, and, importantly, that the assay is suitable for the investigation of the modulation effect of putative activators or blockers on the activity of a chloride transporting protein expressed in the plasma membrane.

Application of the Cl^- flux assay on the gating glutamate mutant E245A. We next tested the assay on the gating glutamate mutant of ClC-7. HEK 293A cells transiently expressing Ostm1-2AP-E245A-ClC-7^{PM}-E^2GFP/DsRed were exposed to a decrease in $[Cl^-]_{ext}$ as described above. A considerable increase of r_{Cl} was observed, comparable to that seen with ClC-1-E^2GFP/DsRed (Fig. 3a). The change of r_{Cl} following the perfusion with the 0 Cl solution was calculated after 100 seconds and is summarized in Fig. 3b.

A remarkable increase of pH related fluorescence is caused by ClC-7 mediated transport driven by the activation of FaNaCh. In a second strategy, we sought to establish a simple assay also for the WT protein by the additional inclusion of a strongly depolarizing agent. K^+ depolarization, but also optogenetic tools, would allow a depolarization to at most 0 mV, insufficient for activation of ClC-7. In contrast, activation of a Na^+ selective channel might provide sufficient positive membrane voltage to drive ClC-7 mediated transport. We thus co-expressed Ostm1-wtClC-7^{PM}-E^2GFP/DsRed with the peptide gated sodium channel FaNaCh, which is specifically activated by the small peptide FMRFamide[31]. A similar strategy has already been employed to activate the depolarization activated CLC-5 transporter[19]. HEK cells co-transfected with the two constructs were tested for functional expression of both Ostm1-2AP-wtClC-7^{PM}-E^2GFP/DsRed and FaNaCh using the patch-clamp technique (data not shown). Despite the relatively large buffer capacity of the cytosol, transport mediated by ClC-7 is expected to produce a larger relative change in the intracellular proton concentration than in the intracellular Cl^- concentration. We thus concentrated on the fluorescence ratio F482/F458 = r_{pH}, which directly reflects changes in pH and is insensitive to changes in Cl^-[24]. Indeed, a striking increase of pH related fluorescence was observable when HEK cells expressing Ostm1-2AP-wtClC-7^{PM}-E^2GFP/DsRed and FaNaCh were perfused with a solution containing FMRFamide (Fig. 4a), while the Cl^- related fluorescence ratio changed only slightly (Supplementary Fig. 3). No change in fluorescence was detected applying the same conditions to cells transfected with Ostm1-2AP-wtClC-7^{PM}-E^2GFP/DsRed but without FaNaCh (Fig. 4b). The change of r_{pH} at 100 seconds after the start of the perfusion with FMRF provides a robust readout of functional ClC-7 activity (Fig. 4c).

Discussion

Plasma membrane ion channels and ion transporters are difficult targets for high-throughput screening assays. Intracellular ion transporters are even more challenging, but these proteins represent an almost untapped class of drug targets. Among these is the lysosomal ClC-7 Cl^- / H^+ antiporter, a promising target to treat osteoporosis[8]. Here we report the development of simple all-optical assays, which provide robust signals of ClC-7/Ostm1 function based on the E^2GFP/DsRed Cl^-/pH sensor. The creation of constructs ensuring the equivalent and simultaneous expression of Ostm1 and ClC-7 in the plasma membrane, employing ClC-7 sorting mutants[17] and self-cleavable peptides[26] successfully solved the problem of the tricky measure of an intracellular membrane protein that compulsorily needs a beta subunit to be active. The fusion of the biosensor to the C-terminus does not modify the functional properties and the 2AP construct is able to mediate the expression of both the Ostm1 and the ClC-7 protein.

We applied two alternative strategies to cope with the problem that the transporter is activated only at large positive voltages. Firstly, we mutated the conserved gating glutamate to alanine which eliminates the voltage dependence and renders ClC-7 a passive Cl^- conductance. For this E245A mutant we established a Cl^- flux assay, which provides a simple readout of the transport function. To test the assay we used the ClC-1 Cl^- channel as a surrogate for which relatively high affinity blocker are available. For this channel the assay provided an accurate and robust readout of the pharmacological sensitivity of the channel.

Since the uncoupling mutant maintains the basic chloride permeation pathway it can be expected that drugs that block the E245A mutant will also inhibit the WT protein with a similar efficacy, but not the other way round. For example, drugs that interfere with the mechanism of the voltage-dependence might block the WT protein but not the uncoupling mutant. We thus sought an alternative assay for the WT transporter. To achieve a sufficient depolarization of the cell we co-expressed ClC-7 together with the peptide gated Na^+ channel FaNaCh, and measured the resulting intracellular alkalinization caused by the Cl^-/H^+ antiport triggered by the application of the FMRF peptide.

Thus, we developed two complementary, all-optical assays for ClC-7 function, ready to be used in a pharmacological screening for ClC-7 inhibitors.

Nevertheless both assays can be further simplified for the adaption in miniaturized HTS assays. A first simplification regards the FaNaCh based assay in which two cDNAs have to be co-transfected and the FaNaCh protein expression is not visually possible. One solution could be the construction of viral vectors to assure a uniform and high-yield FaNaCh expression. Alternatively, the FaNaCh ORF

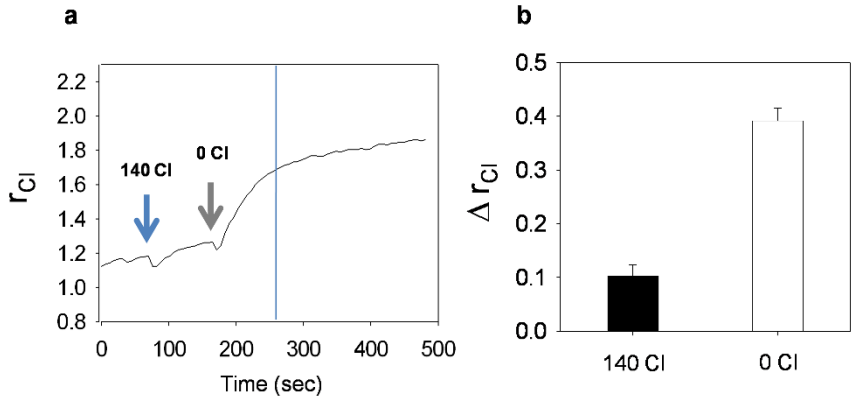

Figure 3 | Cl^- flux assay for the gating glutamate mutant E245A. Effect of the change in $[Cl^-]_{ext}$ from 140 mM to 0 mM on r_{Cl} on a single cell expressing Ostm1-2AP-E245A-ClC-7^{PM}-E^2GFP/DsRed (a). Average values of the change of r_{Cl} at 100 seconds after the start of the perfusion with the indicated solutions (140 Cl: n = 19; 0 Cl: n = 26; Error = SEM) (b).

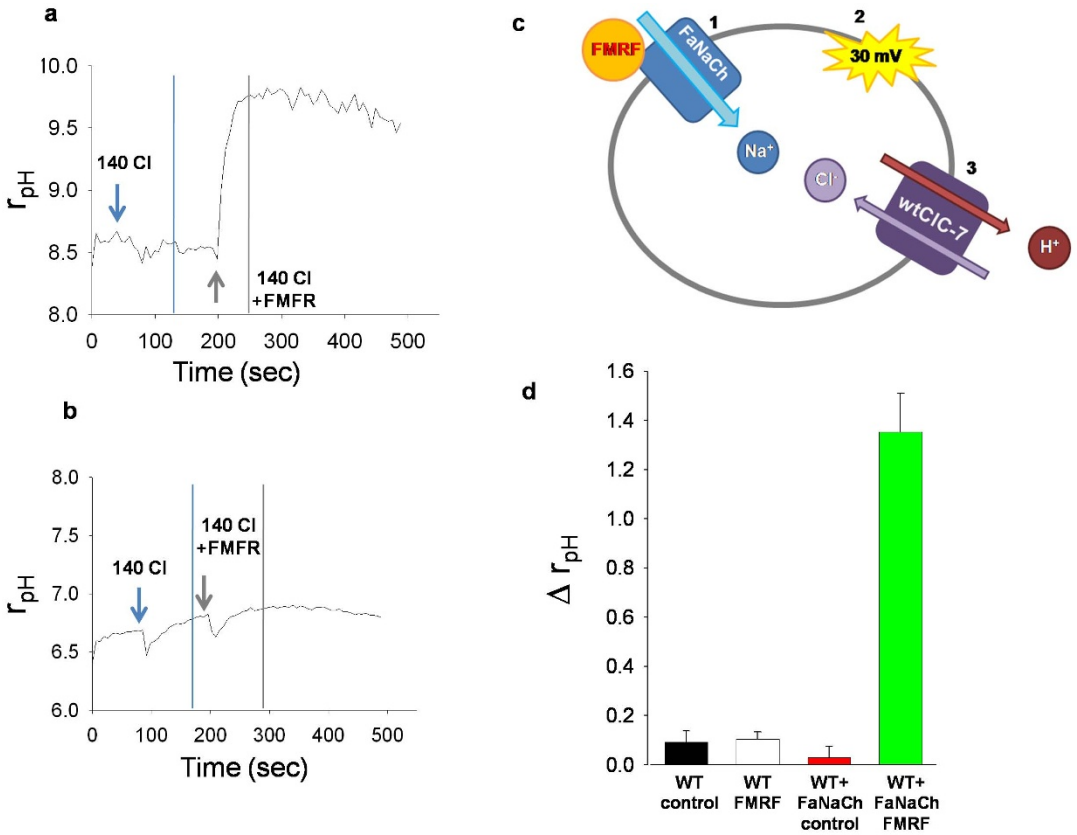

Figure 4 | ClC-7 mediated transport driven by the activation of FaNaCh causes a remarkable increase of pH related fluorescence. Effect of 30 μM FMRF on r_{pH} on single cells expressing Ostm1-2AP-wtClC-7^{PM}-E^2GFP/DsRed and FaNaCh (a) or Ostm1-2AP-wtClC-7^{PM}-E^2GFP/DsRed alone (b). Scheme of the mechanism of the stimulation of ClC-7 transport by FaNaCh activation (c). Mean values of the changes of r_{pH} at 100 seconds after the addition of FMRF (WT control: n = 31; WT FMRF: n = 31; WT+FaNaCh control: n = 24; WT+FaNaCh FMRF: n = 25; Error = SEM) (d).

could be joined onto the Ostm1-2AP-wtClC-7PM-E2GFP/DsRed construct using a second 2A peptide, insuring contemporaneous expression after transient transfection easily revealed by the presence of the E^2GFP/DsRed fluorescence.

Several simplifications of the optical system can be considered for both assays. For the Cl^- flux assay (using the E245A mutant), it is not necessary to record pH changes and thus it is possible eliminate the E^2GFP excitation at the pH sensitive wavelength (482 nm). For the FaNaCh based alkalinization assay it is not necessary to record changes in the chloride concentration, and thus, the excitation and emission of the DsRed fluorescence can be eliminated. Consequently, in this second case it is also possible to simplify the fluorescence sensor eliminating the DsRed part. With these simplifications the assays could for example be implemented on a microplate reader necessitating two excitation frequencies, one or two emission lines and one solution application step for each assay. Applying both assays in parallel has the further advantage that positive hits emerging in one of the assays can be cross validated by the other one, providing hints on the mechanism of action of potential ClC-7 blockers.

Methods

Molecular biology and transient DNA expression. The N-terminal mutant (L23A-L24A-L36A-L37A named ClC-7^{PM}) of rat ClC-7[17,18] with the E^2GFP/DsRed Cl^-/pH sensor[24] fused to the C-terminus[25], mouse Ostm1 and ClC-1-E^2GFP/DsRed (C-term) were in pFrog, a pCDNA3 derived vector suitable for transient expression in HEK293 cells. The E245A mutant of ClC-7 was introduced into the background of ClC-7^{PM}-E^2GFP/DsRed-pFROG[25]. In new constructs we fused Ostm1 and ClC-7^{PM}-E^2GFP/DsRed or ClC-7^{PM}-E245A-E^2GFP/DsRed using the 2A peptide sequence coded by GGCAGTGGAGAGGGCAGAGGAAGTCTGCTAACATGCGGTGACGTCGA GGAGAATCCTGGCCCA[26]. To this end we designed two overlapping 60 bp long primers. The forward primer started with the last two thirds of the 2AP sequence (in bold in the primer sequence) and ended with the 21 starting bases of ClC-7 (in italic in the primer sequence) (2AP-rC7E^2GFPDsRed_F: **GTCTGCTAACATGCG GTGACGTCGAGGAGAATCCTGGCCCA***ATGGCCAACGTTTCTAAGAA*). The reverse primer partially overlapped the forward primer (underlined) in the 2AP part (bold) and included the 21 final bases of Ostm1 (in italic), excluding the stop codon (2Ap-OSTM1_R: **CACCGCATGTTAGCAGACTTCCTCTGCCCTC TCCACTGCC***GGTGGCATTTTCTTGAATGT*). These two primers were used in separate reactions with external primers within Ostm1 and ClC-7 respectively and the two PCR products were combined in a recombinant PCR employing the external primers. The resulting PCR-product was inserted into pFROG with specific restriction reactions in frame with Ostm1 and ClC-7^{PM}-E^2GFP/DsRed.

The original clones of ClC-7 and Ostm1 were kindly provided by T.J. Jentsch. FaNaCh from *Helix asperga* in the pBSK vector was obtained from E. Lingueglia.

Transient transfection in HEK293 cells was performed using the Effectene Transfection Reagent Kit (Qiagen, cat. # 301425) according to manufacturer's instructions. For oocyte expression the same constructs were cloned into the PTLN vector[33]. All constructs were expressed by injecting 25–50 ng of cRNA transcribed from linearized cDNA using the Ambion mMessage mMachine SP6 kit. Oocytes maintenance solution contained (in mM) 90 NaCl, 10 HEPES, 2 KCl, 1 $MgCl_2$, 1 $CaCl_2$, pH 7.5. Oocytes were kept at 18 °C for 3–6 days.

Cell Growth and Harvesting. HEK 293 cells were purchased from Invitrogen and maintained in 25 cm^2 flasks in a cell growth medium composed of 90% D-MEM high-glucose, Na-Pyruvate and L-Glutamine (Euroclone, ECM0728L), 10% FBS (Sigma), 1% Pen-Strep (Sigma). For fluorescence measurements, cells were seeded on polylysine treated 3 cm diameter glass-bottom petri dish chambers. These dishes were manufactured in the IBF Mechanical Workshop by gluing a round 22 mm diameter cover glass to a holed petri dish using Sylgard.

Electrophysiology. In accordance with national guidelines, oocytes were collected from *Xenopus* females anaesthetized with tricaine. After surgery, frogs were allowed to recover from anesthesia and suitable aftercare was given. For two-electrode voltage clamp recordings, the standard extracellular solution contained (in mM): 100 NaCl, 5 $MgSO_4$, 10 Hepes, pH 7.3. Chloride was changed by substitution of NaCl with NaGlutamate. For all the recordings the pulse protocol consisted of voltage steps of 100 ms from −140 to 60 mV with 20 mV increments from a holding potential of −20 mV, preceded by a 50 ms conditioning prepulse to 60 mV and followed by a 50 ms postpulse to −100 mV. For patch-clamp the standard extracellular solutions

contained (in mM)(Gluc = Gluconate): 140 Cl solution: 140 NaCl, 2 $MgSO_4$, 2 $CaCl_2$, and 10 HEPES/NaOH (pH 7.3). 0 Cl solution: 140 mM NaGluc, 3 $MgSO_4$, 2 CaGluc, 10 HEPES/NaOH (pH 7.3). Intracellular solution was (in mM) 130 NaCl, 2 $MgSO_4$, 2 EGTA, and 10 HEPES/NaOH (pH 7.3). All recordings were performed in the whole-cell configuration using an EPC7 amplifier and the custom data acquisition program GePulse.

Fluorescence assay. The optical system is composed of a basic iMIC microscope with a QImaging Retiga EXI Blue camera and a dual-view port for the emission allowing the separation of the GFP and DsRed emissions (Till Photonics). For excitation we used Till Oligochrome a wavelength-switching device containing a stable Xenon light-source. Because of a slight imperfection, likely to be caused by a mechanical slip of the petri dish in the microscope fitting, the localization of the cells was slightly variable during time. This problem was resolved by adjusting our (self written) analysis software, developing a simple tracking feature. In this way up to 15 cells could be assayed in parallel for a single application of substances. The transfected cells were exposed to a change in $[Cl^-]_{ext}$ (140 Cl solution: 138 mM NaCl, 2 KCl, 10 Hepes, 10 Glucose, 3 $MgSO_4$,1.8 $CaCl_2$, Mannitol 100 mM, Valinomycin 200 μM; 0 Cl solution: 140 mM NaGluc, 2 CaGluc, 10 Hepes, 10 Glucose, 3 $MgSO_4$, Mannitol 100 mM, Valinomycin 100 μM while excited at 458 nm (100 msec exposition), 482 nm (30 msec exposition) and 563 nm (100 msec exposition). The iMIC filter GFP/DsRed and iMIC dichroic GFP/DsRed were used for all the acquisitions. The specific ClC-1 blocker, 9-AC was dissolved in DMSO and added to the solution to the desired concentration (DMSO <= 0.1 %). For the experiments requiring FaNaCh activation, 30 μM FMRFamide was added to the 140 Cl solution. The pH of all solutions was titrated to 7.3. For the analysis we defined: rCl = F458/F563 and r_{pH} = F482*3.33/F458. The factor 3.33 stems from the 3.33 fold shorter exposition at the (brighter) 482 excitation wavelength. Data analysis was performed with the custom analysis programs Anavision and Ana (freely available at http://users.ge.ibf.cnr.it/pusch). A region of interest was drawn on the border of the analyzed cell and another on the background for background subtraction. Figures were prepared using SigmaPlot software.

1. Woolf, A. D. & Pfleger, B. Burden of major musculoskeletal conditions. *Bull World Health Organ* **81**, 646–656 (2003).
2. Raisz, L. G. Pathogenesis of osteoporosis: concepts, conflicts, and prospects. *J. Clin. Invest.* **115**, 3318–3325 (2005).
3. Teitelbaum, S. L. Bone resorption by osteoclasts. *Science* **289**, 1504–1508 (2000).
4. Baron, R., Neff, L., Louvard, D. & Courtoy, P. J. Cell-mediated extracellular acidification and bone resorption: evidence for a low pH in resorbing lacunae and localization of a 100-kD lysosomal membrane protein at the osteoclast ruffled border. *J Cell Biol* **101**, 2210–2222 (1985).
5. Weinert, S. *et al*. Lysosomal pathology and osteopetrosis upon loss of H^+-driven lysosomal Cl^- accumulation. *Science* **328**, 1401–1403 (2010).
6. Silverman, S. & Christiansen, C. Individualizing osteoporosis therapy. *Osteoporosis International* **23**, 797–809 (2012).
7. Kennel, K. A. & Drake, M. T. Adverse effects of bisphosphonates: implications for osteoporosis management. *Mayo Clin. Proc.* **84**, 632–637 (2009).
8. Schaller, S. *et al*. The chloride channel inhibitor NS3736 [corrected] prevents bone resorption in ovariectomized rats without changing bone formation. *J. Bone Miner. Res.* **19**, 1144–1153 (2004).
9. Chalhoub, N. *et al*. Grey-lethal mutation induces severe malignant autosomal recessive osteopetrosis in mouse and human. *Nat. Med.* **9**, 399–406. (2003).
10. Kasper, D. *et al*. Loss of the chloride channel ClC-7 leads to lysosomal storage disease and neurodegeneration. *Embo. J.* **24**, 1079–1091 (2005).
11. Kornak, U. *et al*. Loss of the ClC-7 chloride channel leads to osteopetrosis in mice and man. *Cell* **104**, 205–215 (2001).
12. Lange, P. F., Wartosch, L., Jentsch, T. J. & Fuhrmann, J. C. ClC-7 requires Ostm1 as a beta-subunit to support bone resorption and lysosomal function. *Nature* **440**, 220–223 (2006).
13. Pressey, S. N. *et al*. Distinct neuropathologic phenotypes after disrupting the chloride transport proteins ClC-6 or ClC-7/Ostm1. *J Neuropathol Exp Neurol* **69**, 1228–1246.
14. Accardi, A., Kolmakova-Partensky, L., Williams, C. & Miller, C. Ionic currents mediated by a prokaryotic homologue of CLC Cl^- channels. *J. Gen. Physiol.* **123**, 109–119. (2004).
15. Zifarelli, G. & Pusch, M. CLC chloride channels and transporters: a biophysical and physiological perspective. *Rev. Physiol. Biochem. Pharmacol.* **158**, 23–76 (2007).
16. Jentsch, T. J. CLC chloride channels and transporters: from genes to protein structure, pathology and physiology. *Crit. Rev. Biochem. Mol. Biol.* **43**, 3–36 (2008).
17. Stauber, T. & Jentsch, T. J. Sorting motifs of the endosomal/lysosomal CLC chloride transporters. *J. Biol. Chem.* **285**, 34537–34548 (2010).
18. Leisle, L., Ludwig, C. F., Wagner, F. A., Jentsch, T. J. & Stauber, T. ClC-7 is a slowly voltage-gated 2Cl(−)/1H(+)-exchanger and requires Ostm1 for transport activity. *Embo J* **30**, 2140–2152 (2011).
19. Scheel, O., Zdebik, A. A., Lourdel, S. & Jentsch, T. J. Voltage-dependent electrogenic chloride/proton exchange by endosomal CLC proteins. *Nature* **436**, 424–427 (2005).
20. Picollo, A. & Pusch, M. Chloride/proton antiporter activity of mammalian CLC proteins ClC-4 and ClC-5. *Nature* **436**, 420–423 (2005).
21. Accardi, A. & Miller, C. Secondary active transport mediated by a prokaryotic homologue of ClC Cl^- channels. *Nature* **427**, 803–807 (2004).
22. De Angeli, A. *et al*. The nitrate/proton antiporter AtCLCa mediates nitrate accumulation in plant vacuoles. *Nature.* **442**, 939–942. (2006).
23. Jensen, V. K. *et al*. A quantitative assay for lysosomal acidification rates in human osteoclasts. *Assay Drug Dev Technol* **9**, 157–164 (2011).
24. Arosio, D. *et al*. Simultaneous intracellular chloride and pH measurements using a GFP-based sensor. *Nat. Methods* **7**, 516–518 (2010).
25. Costa, A. *et al*. The Arabidopsis central vacuole as an expression system for intracellular transporters: functional characterization of the Cl−/H+ exchanger CLC-7. *J Physiol* **590**, 3421–3430 (2012).
26. Trichas, G., Begbie, J. & Srinivas, S. Use of the viral 2A peptide for bicistronic expression in transgenic mice. *BMC Biol* **6**, 40 (2008).
27. Liantonio, A. *et al*. Molecular switch for CLC-K Cl^- channel block/activation: Optimal pharmacophoric requirements towards high-affinity ligands. *Proc. Natl. Acad. Sci. U. S. A.* **105**, 1369–1373 (2008).
28. Steinmeyer, K. *et al*. Inactivation of muscle chloride channel by transposon insertion in myotonic mice. *Nature* **354**, 304–308 (1991).
29. Estévez, R., Schroeder, B. C., Accardi, A., Jentsch, T. J. & Pusch, M. Conservation of chloride channel structure revealed by an inhibitor binding site in ClC-1. *Neuron* **38**, 47–59 (2003).
30. Eggermont, J., Trouet, D., Carton, I. & Nilius, B. Cellular function and control of volume-regulated anion channels. *Cell. Biochem. Biophys.* **35**, 263–274 (2001).
31. Lingueglia, E., Champigny, G., Lazdunski, M. & Barbry, P. Cloning of the amiloride-sensitive FMRFamide peptide-gated sodium channel. *Nature* **378**, 730–733 (1995).
32. Liantonio, A. *et al*. Molecular requisites for drug binding to muscle CLC-1 and renal CLC-K channel revealed by the use of phenoxy-alkyl derivatives of 2-(p- chlorophenoxy)propionic acid. *Mol. Pharmacol.* **62**, 265–271 (2002).
33. Lorenz, C., Pusch, M. & Jentsch, T. J. Heteromultimeric CLC chloride channels with novel properties. *Proc. Natl. Acad. Sci. U. S. A.* **93**, 13362–13366 (1996).

Acknowledgements

We thank D. Arosio for the E^2GFP/DsRed clone, T.J. Jentsch for the WT clones of ClC-7 and Ostm1, E. Lingueglia for the FaNaCh clone, A. Gradogna and S. De Stefano for help with the oocyte injection, A. Liantonio and D. Conte Camerino for sharing chloride channel blockers, and F. Quartino, A. Barbin, and D. Magliozzi for technical assistance. The financial support by the Italian Institute of Technology (progetto SEED), Telethon Italy (grant GGP12008), the Italian Ministry of Education (progetto PRIN), and the Compagnia San Paolo is gratefully acknowledged.

Author contributions

M.P. and G.Z. conceived the project. M.P. and I.Z. planned and performed the experiments, analyzed the data, and wrote the manuscript.

Additional information

Supplementary information accompanies this paper at http://www.nature.com/scientificreports

Competing financial interests: The authors declare no competing financial interests.

How to cite this article: Zanardi, I., Zifarelli, G. & Pusch, M. An optical assay of the transport activity of ClC-7. *Sci. Rep.* **3**, 1231; DOI:10.1038/srep01231 (2013).